

Library Copy
R.A. 1700

UNCLASSIFIED

Copy No. 45
RM No. SL8107

~~CONFIDENTIAL~~

SEP 28 1947

NACA

RESEARCH MEMORANDUM

for the

Air Materiel Command, U. S. Air Force

A THEORETICAL LATERAL-STABILITY ANALYSIS
OF XC-120 AIRPLANE

By

Leonard Sternfield and Ordway B. Gates, Jr.

Langley Aeronautical Laboratory
Langley Field, Va.

CLASSIFICATION CHANGED

To: ~~Confidential~~
RF # 209.1
20 to 50

By authority of ~~J. M. Cassin~~
Date 12/1/53
JH-1-25-54

CLASSIFICATION CANCELLED

Authority ~~RF # 209.1~~ R 7-2793 Date 11/1/53

By ~~JH-1-24-55~~ See

CLASSIFIED DOCUMENT

This document contains classified information affecting the National Defense of the United States within the meaning of the Espionage Act, USC 50:41 and 42. Its transmission or the revelation of its contents in any manner to an unauthorized person is prohibited by law. Information so classified may be imparted only to persons in the military and naval services of the United States, appropriate civilian officers and employees of the Federal Government who have a legitimate interest therein, and to United States citizens of known loyalty and discretion who of necessity must be informed thereof.

NATIONAL ADVISORY COMMITTEE FOR AERONAUTICS

WASHINGTON

NACA LIBRARY
LANGLEY MEMORIAL AERONAUTICAL
LABORATORY
Langley Field, Va.

Inactive per each memo
3/11/57 MHA 3/21/55

~~CONFIDENTIAL~~

UNCLASSIFIED



UNCLASSIFIED

NATIONAL ADVISORY COMMITTEE FOR AERONAUTICS

RESEARCH MEMORANDUM

for the

Air Materiel Command, U. S. Air Force

A THEORETICAL LATERAL-STABILITY ANALYSIS

OF XC-120 AIRPLANE

By Leonard Sternfield and Ordway B. Gates, Jr.

SUMMARY

A theoretical lateral-stability analysis of the XC-120 airplane, equipped with a detachable fuselage, was made to determine the effect on the lateral stability of the high angle of wing incidence for which the airplane was designed. The results of the investigation indicated that the lateral stability of the airplane is satisfactory with or without the detachable fuselage installed.

INTRODUCTION

At the request of the Air Materiel Command, U. S. Air Force, a theoretical lateral-stability analysis of the XC-120 airplane was carried out to determine the effect on the lateral stability of the high angle of wing incidence, for which this airplane was designed.

The XC-120 is a twin-engine cargo-type airplane and is equipped with a detachable fuselage which may be used for transporting cargo, litters, or air-borne troops. Because of the rapid detachability of the fuselage, the airplane has the advantage of not being delayed by loading operations. The XC-120 is intended to have satisfactory lateral stability with or without the detachable fuselage installed and therefore both configurations were included in the analysis. A three-view sketch of the XC-120 airplane is presented in figure 1.

The lateral-stability calculations were made by use of the general purpose computing system of the Bell Telephone Laboratories for the landing and cruising conditions and the results were analyzed in the Stability Analysis Section.

UNCLASSIFIED

RESTRICTED

SYMBOLS AND COEFFICIENTS

ϕ	angle of bank, radians
ψ	angle of azimuth, radians
β	angle of sideslip, radians
V	airspeed, feet per second
ρ	mass density of air, slugs per cubic foot
q	dynamic pressure, pounds per square foot $\left(\frac{1}{2}\rho V^2\right)$
b	wing span, feet
S	wing area, square feet
l_t	distance from center of gravity of airplane to center of pressure of vertical tail, feet
\bar{z}	height of center of pressure of vertical tail above fuselage axis, feet
W	weight of airplane, pounds
m	mass of airplane, slugs (W/g)
g	acceleration of gravity, feet per second per second
μ	relative-density factor $(m/\rho S b)$
η	angle of attack of principal longitudinal axis of airplane, positive when principal axis is above flight path at the nose, degrees
α	angle of attack of fuselage center line, degrees
k_{X_0}	radius of gyration in roll about principal longitudinal axis, feet
k_{Z_0}	radius of gyration in yaw about principal normal axis, feet
C_L	trim lift coefficient (W/qS)

- $C_{l\beta}$ effective-dihedral derivative, rate of change of yawing-moment coefficient with angle of sideslip, per radian $(\partial C_l / \partial \beta)$
- $C_{n\beta}$ directional-stability derivative, rate of change of yawing-moment coefficient with angle of sideslip, per radian $(\partial C_n / \partial \beta)$
- $C_{Y\beta}$ lateral-force derivative, rate of change of lateral-force coefficient with angle of sideslip, per radian $(\partial C_Y / \partial \beta)$
- C_{nr} damping-in-yaw derivative, rate of change of yawing-moment coefficient with yawing-angular-velocity factor, per radian $\left(\frac{\partial C_n}{\partial \frac{rb}{2V}} \right)$
- C_{np} rate of change of yawing-moment coefficient with rolling-angular-velocity factor, per radian $\left(\frac{\partial C_n}{\partial \frac{pb}{2V}} \right)$
- C_{lr} damping-in-roll derivative, rate of change of rolling-moment coefficient with rolling-angular-velocity factor, per radian $\left(\frac{\partial C_l}{\partial \frac{pb}{2V}} \right)$
- C_{lr} rate of change of rolling-moment coefficient with yawing-angular-velocity factor, per radian $\left(\frac{\partial C_l}{\partial \frac{rb}{2V}} \right)$
- t time, seconds
- λ_1, λ_2 real roots of characteristic stability equation
- $\lambda_{3,4}$ complex roots of characteristic stability equation
- P period of oscillation, seconds
- $T_{1/2}$ time for amplitude of periodic or aperiodic mode to change by factor of 2 (positive value indicates a decrease to half amplitude, negative value indicates an increase to double amplitude)

$C_{l/2}$ number of cycles required for amplitude of periodic mode to change by factor of 2 (positive value indicates a decrease to half amplitude; negative value indicates an increase to double amplitude)

Scope of Investigation

The oscillatory- and spiral-stability boundaries were calculated for the airplane, with and without the detachable fuselage, in both the cruising and landing conditions. The calculations were based on the lateral-stability equations presented in reference 1. The values of the stability derivatives and mass characteristics used in the calculations were obtained from data furnished by the Fairchild Engine and Airplane Corporation, and are presented in table I. Cases Ia and IIa represent the airplane cruising at maximum speed at an altitude of 18,000 feet, whereas in cases Ib and IIb the airplane was assumed cruising at the speed and altitude necessary for maximum range. Cases IIIa and IVa represent the airplane with landing gear extended, wing flaps deflected 40° , 80 percent of the fuel expended, flying at an airspeed in the vicinity of the design airspeed of the wing flap at sea level. Cases IIIb and IVb are comparable to IIIa and IVa except that the airplane is assumed flying at a speed near the stalling speed.

The period and time to damp to half amplitude of the oscillatory mode and the time to damp to half amplitude of the aperiodic modes of motion were determined from the roots of the fourth degree lateral-stability equation. The roots were calculated for each of the cases presented in table I, using the estimated values of $C_{n\beta}$ and $C_{l\beta}$ of the airplane as presently designed and also using the $C_{n\beta}$, $C_{l\beta}$ values obtained from wind-tunnel tests of the C-82 airplane corrected to the XC-120 airplane.

For three of the cases presented in table I, namely cases IIa, IIb, and IVb, selected from an analysis of the period and damping relationship of the oscillatory mode and the damping of the aperiodic modes, additional calculations were made in order to determine the motion of the airplane in bank, yaw, and sideslip, subsequent to an initial displacement in bank or sideslip.

Results and Discussions

Stability boundaries.— Figures 2(a) and 2(b) show the neutral oscillatory-stability and spiral-stability boundaries for the cases of cruising and landing flight, respectively, plotted as a function of the directional-stability derivative $C_{n\beta}$ and the effective-dihedral derivative $C_{l\beta}$. The $R = 0$ curves of each figure represent the neutral oscillatory-stability boundaries and the $E = 0$ curves represent the

spiral-stability boundaries. The $C_{n\beta}$, $C_{l\beta}$ combinations of the airplane for the conditions described in table I are located within the region indicated by the hatched rectangles in figures 2(a) and 2(b). A primary purpose of this theoretical investigation was to determine the effect of the 7° wing incidence of the XC-120 on the lateral stability of the airplane. Previous investigations (references 1 and 2) have shown that positive wing incidence may have a pronounced adverse effect on the oscillatory stability. This adverse effect is due to the fact that for a given flight condition, the principal longitudinal axis of an airplane with positive wing incidence would be located below that of the airplane with no wing incidence. The effect of the location of the principal longitudinal axis on the oscillatory stability is reflected in the magnitude of the nondimensional product-of-inertia parameter $\mu \left(\frac{k_{z_0}^2 - k_{x_0}^2}{b^2} \right) \sin \eta \cos \eta$. However,

for the cases considered in this investigation, the location of the principal longitudinal axis varied from 6° above (cases IIIb and IVb) to 7° below the flight path (case IVa) with no large destabilizing shift occurring in the oscillatory-stability boundaries. It is seen from figures 2(a) and 2(b) that the XC-120 airplane would be oscillatorily stable for almost any combination of $C_{n\beta}$ and $C_{l\beta}$ in the first quadrant. This negligible effect of the location of the principal longitudinal axis with respect to the flight path on the oscillatory stability of this particular airplane can be attributed to the small value of the relative-density factor μ and to the small value of the term $\frac{k_{z_0}^2 - k_{x_0}^2}{b^2}$.

Roots of the lateral-stability quartic equation.— For each of the cases presented in table I, roots of the lateral-stability quartic equation were calculated by using the estimated values of $C_{n\beta}$ and $C_{l\beta}$, and also by using the $C_{n\beta}$, $C_{l\beta}$ values obtained from wind-tunnel tests of the C-82 airplane corrected to apply to the XC-120 airplane. The roots of the stability equation for each of the cases considered are two real roots and a pair of conjugate complex roots. One of the real roots λ_1 corresponds to the heavy damping of the pure rolling motion; whereas, the other real root λ_2 , which is numerically small, corresponds to the spiral mode. The pair of conjugate complex roots with the real part negative $\lambda_{3,4}$ represents the stable oscillatory mode. The time to damp to half amplitude for the aperiodic modes $(T_{1/2})_{\lambda_1}$ and $(T_{1/2})_{\lambda_2}$, and the period P time to damp to half amplitude,

$(T_{1/2})_{\lambda_{3,4}}$, and the number of cycles required to damp to half

amplitude $C_{1/2}$ for the oscillatory mode are presented in table II for each of the cases investigated. The results of $(T_{1/2})_{\lambda_1}$ clearly show

that for every case this mode of motion is very heavily damped. In the extreme case (case IVb), only 0.4 of a second is required for the motion to damp to half amplitude. The excellent damping characteristics of this mode are due to the large value of the damping-in-roll derivative $C_{\lambda_p} = -0.49$. From an analysis of the spiral roots λ_2 it is seen

that for cases Ib, IIb, IIIb, and IVb the airplane is spirally unstable. For the extreme cases, IIb (cruising) and IVb (landing), the times required for the amplitude of the spiral divergence to double are approximately 21 seconds and 8 seconds, respectively. The effect of this spiral instability on the airplane motions is discussed in the following section entitled, "Lateral motions of airplane." The period and damping relationship of the oscillatory mode, $\lambda_{3,4}$, appears to be very satisfactory for every case investigated. The number of cycles required for the oscillation to damp to half amplitude $C_{1/2}$ varies from 0.29 (case IIIb) to 0.85 (case IIa).

Lateral motions of airplane.— In order to present a more complete stability analysis of the XC-120 airplane, additional calculations were made to determine the motion of the airplane in bank, yaw, and sideslip, subsequent to an initial displacement in bank or sideslip, for three of the cases investigated, namely cases IIa, IIb, and IVb. These motions were calculated by using the values of $C_{n\beta}$ and $C_{\lambda\beta}$ obtained from wind-tunnel tests of the C-82 airplane corrected to apply to the XC-120 airplane. Although the period and damping relationship of case IIa ($C_{1/2} = 0.85$) was considered satisfactory and the spiral instability of cases IIb and IVb was not believed to be serious, the motions for cases IIa, IIb, and IVb were calculated because it was felt that these cases would be indicative of the worst possible conditions likely to be encountered in any of the cases investigated. The magnitude of the displacement was arbitrarily assumed to be 5° . Since the lateral equations used in the calculation of the motion are linear, the amplitudes of the resultant motions are directly proportional to the magnitudes of the displacements. A comparison of figures 3 to 5 shows that the oscillatory mode is predominant in the motions obtained subsequent to a displacement in sideslip. As indicated by the $C_{1/2}$ values for cases IIa, IIb, and IVb, figures 3(b), 4(b), and 5(b) show that the damping of the oscillation increases as $C_{1/2}$ is reduced. The effect of the spiral instability is more clearly seen from a comparison of figures 3(a), 4(a), and 5(a). As the spiral instability of the airplane increases, the rate of divergence of the angles of yaw and bank also increases. However, because of the slow rate of divergence, the pilot should not find this type of instability difficult to control.

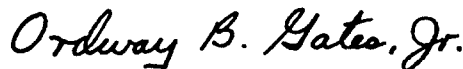
CONCLUSIONS

The results of the theoretical lateral-stability analysis of the XC-120 airplane indicated that the lateral stability of the airplane was satisfactory with or without the detachable fuselage installed.

Langley Aeronautical Laboratory
National Advisory Committee for Aeronautics
Langley Field, Va.



Leonard Sternfield
Aeronautical Research Scientist



Ordway B. Gates, Jr.
Aeronautical Research Scientist

Approved:



Thomas A. Harris
Chief of Stability Research Division

cgb

REFERENCES

1. Sternfield, Leonard: Effect of Product of Inertia on Lateral Stability. NACA TN No. 1193, 1947.
2. McKinney, Marion O., Jr., and Drake, Hubert M.: Correlation of Experimental and Calculated Effects of Product of Inertia on Lateral Stability. NACA TN No. 1370, 1947.

TABLE I
MASS CHARACTERISTICS AND STABILITY DERIVATIVES

	Cruising condition				Landing condition			
	Fuselage on		Fuselage off		Fuselage on		Fuselage off	
	Case Ia	Case Ib	Case IIa	Case IIb	Case IIIa	Case IIIb	Case IVa	Case IVb
Weight, lb	64,000	64,000	52,425	52,425	52,000	52,000	38,964	38,964
Altitude, ft	18,000	10,000	18,000	10,000	0	0	0	0
V, ft/sec	359	205	390	205	220	137.4	220	118.9
S, ft ²	1447	1447	1447	1447	1447	1447	1447	1447
b, ft	109	109	109	109	109	109	109	109
μ	9.24	7.17	7.58	5.87	4.29	4.29	3.22	3.22
CL	0.505	1.20	0.35	0.982	0.624	1.60	0.468	1.60
η, deg	-3.41	4.79	-6.13	1.47	-5.26	6.22	-7.03	6.22
α, deg	-2.0	6.2	-4.0	3.6	-4.75	6.75	-6.5	6.75
l _t /b	0.40	0.40	0.40	0.40	0.40	0.40	0.40	0.40
Z/b	0.0456	0.0456	0.0456	0.0456	0.0456	0.0456	0.0456	0.0456
k _{X0} , ft	15.49	15.49	16.87	16.87	14.04	14.04	15.98	15.98
k _{Z0} , ft	19.68	19.68	21.30	21.30	18.50	18.50	20.82	20.82
C _{l_p} , per radian	-0.49 + C _{l_p} (tail)	-0.49 + C _{l_p} (tail)	-0.49 + C _{l_p} (tail)	-0.49 + C _{l_p} (tail)	-0.49 + C _{l_p} (tail)	-0.49 + C _{l_p} (tail)	-0.49 + C _{l_p} (tail)	-0.49 + C _{l_p} (tail)
C _{n_β} , per radian	-0.07 + C _{n_β} (tail)	-0.073 + C _{n_β} (tail)	-0.057 + C _{n_β} (tail)	-0.059 + C _{n_β} (tail)	-0.068 + C _{n_β} (tail)	-0.072 + C _{n_β} (tail)	-0.055 + C _{n_β} (tail)	-0.06 + C _{n_β} (tail)
C _{n_p} , per radian	-0.028 + C _{n_p} (tail)	-0.067 + C _{n_p} (tail)	-0.019 + C _{n_p} (tail)	-0.055 + C _{n_p} (tail)	-0.03 + C _{n_p} (tail)	-0.084 + C _{n_p} (tail)	-0.022 + C _{n_p} (tail)	-0.084 + C _{n_p} (tail)
C _{n_r} , per radian	-0.0064 + C _{n_r} (tail)	-0.012 + C _{n_r} (tail)	-0.0042 + C _{n_r} (tail)	-0.019 + C _{n_r} (tail)	-0.0054 + C _{n_r} (tail)	-0.034 + C _{n_r} (tail)	-0.004 + C _{n_r} (tail)	-0.034 + C _{n_r} (tail)
C _{Y_β} , per radian	-0.502 + C _{Y_β} (tail)	-0.502 + C _{Y_β} (tail)	-0.273 + C _{Y_β} (tail)	-0.273 + C _{Y_β} (tail)	-0.502 + C _{Y_β} (tail)	-0.502 + C _{Y_β} (tail)	-0.273 + C _{Y_β} (tail)	-0.273 + C _{Y_β} (tail)
C _{l_r} , per radian	0.11 + C _{l_r} (tail)	0.27 + C _{l_r} (tail)	0.072 + C _{l_r} (tail)	0.225 + C _{l_r} (tail)	0.097 + C _{l_r} (tail)	0.319 + C _{l_r} (tail)	0.061 + C _{l_r} (tail)	0.319 + C _{l_r} (tail)

Tail contributions are determined from the following equations:



$$C_{n_{\beta}(\text{tail})} = -\frac{l_t}{b} C_{Y_{\beta}(\text{tail})}; \quad C_{n_r(\text{tail})} = -2 \frac{l_t}{b} C_{n_{\beta}(\text{tail})}$$

$$C_{n_p(\text{tail})} = C_{l_r(\text{tail})} = 2 \left(\frac{Z}{b} - \frac{l_t}{b} \sin \alpha \right) C_{n_{\beta}(\text{tail})}; \quad C_{l_p(\text{tail})} = -2 \frac{b}{l_t} \left(\frac{Z}{b} - \frac{l_t}{b} \sin \alpha \right)^2 C_{n_{\beta}(\text{tail})}$$

TABLE II
DAMPING OF APERIODIC MODE AND DAMPING-PERIOD RELATIONSHIP OF
OSCILLATORY MODE OF MOTION

Case	$C_{n\beta}$	$C_{l\beta}$	$C_{Y\beta}$	$(T_{1/2})_{\lambda_1}$	$(T_{1/2})_{\lambda_2}$	$P_{\lambda_{3,4}}$	$(T_{1/2})_{\lambda_{3,4}}$	$(C_{1/2})_{\lambda_{3,4}}$
Estimated values of $C_{n\beta}$, $C_{l\beta}$, and $C_{Y\beta}$								
Ia	0.062	-0.089	-0.83	0.31	127.3	5.67	3.77	0.66
Ib	.059	-.068	-.83	.42	-23.1	8.05	3.85	.48
IIa	.092	-.089	-.65	.28	298.8	4.34	3.47	.80
IIb	.089	-.070	-.64	.41	-20.7	6.82	3.95	.58
IIIa	.063	-.097	-.83	.20	52.4	5.83	2.73	.47
IIIb	.058	-.066	-.83	.32	-14.5	8.52	2.44	.29
IVa	.092	-.096	-.64	.11	87.2	4.82	3.23	.67
IVb	.088	-.061	-.64	.36	-8.8	7.95	2.47	.31
$C_{n\beta}$, $C_{l\beta}$, and $C_{Y\beta}$ values obtained from wind-tunnel tests of C-82 corrected to the XC-120								
Ia	0.059	-0.089	-0.69	0.31	104.4	5.79	4.05	0.70
Ib	.070	-.068	-.80	.42	-19.1	7.52	3.84	.51
IIa	.084	-.089	-.44	.28	176.9	4.54	3.85	.85
IIb	.096	-.070	-.55	.41	-19.4	6.61	4.01	.61
IIIa	.053	-.097	-.65	.20	34.0	6.27	2.66	.42
IIIb	.070	-.066	-.81	.32	-12.1	7.85	2.29	.29
IVa	.079	-.096	-.42	.11	51.6	5.21	4.09	.78
IVb	.10	-.061	-.58	.36	-8.1	7.54	2.47	.33



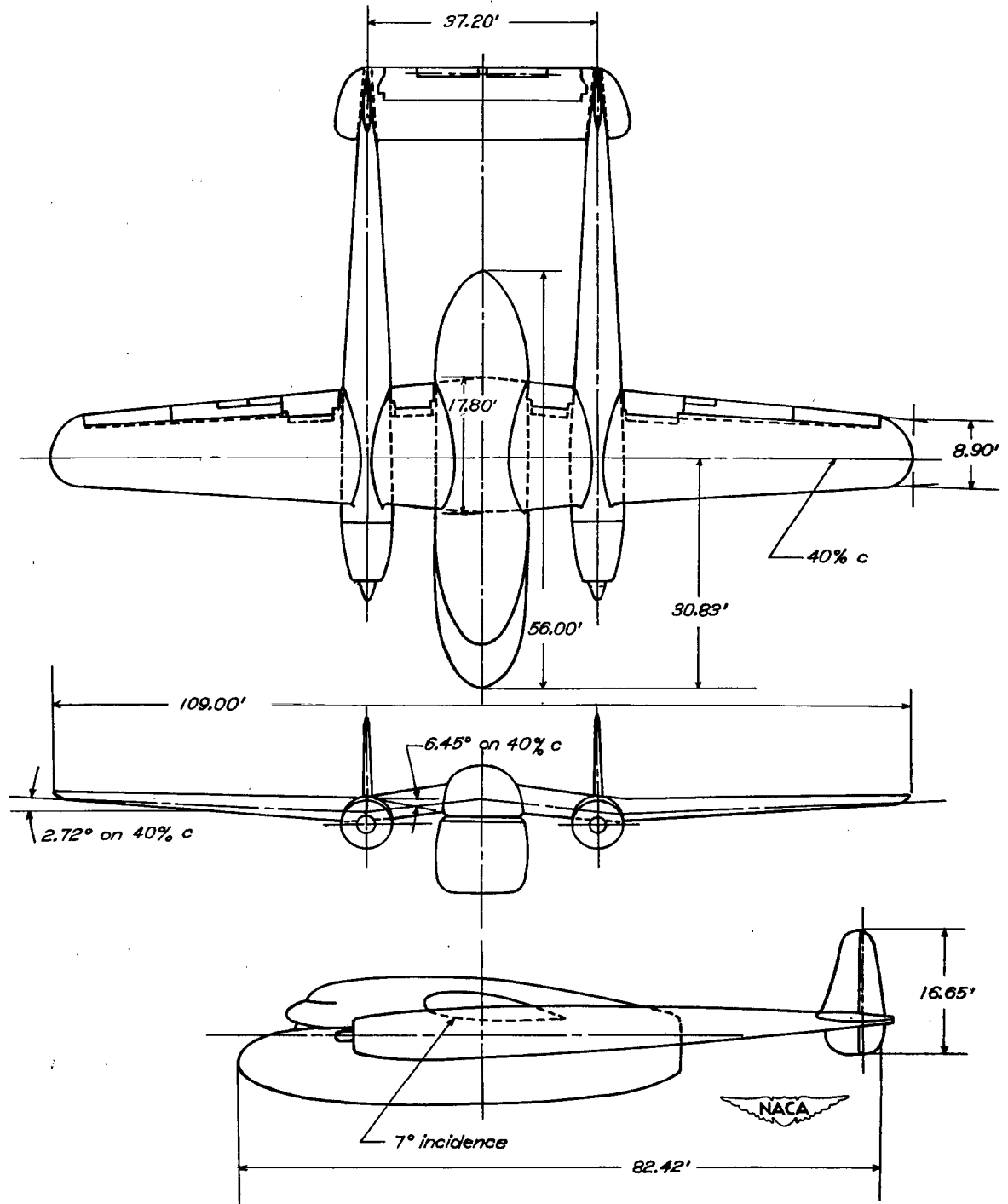
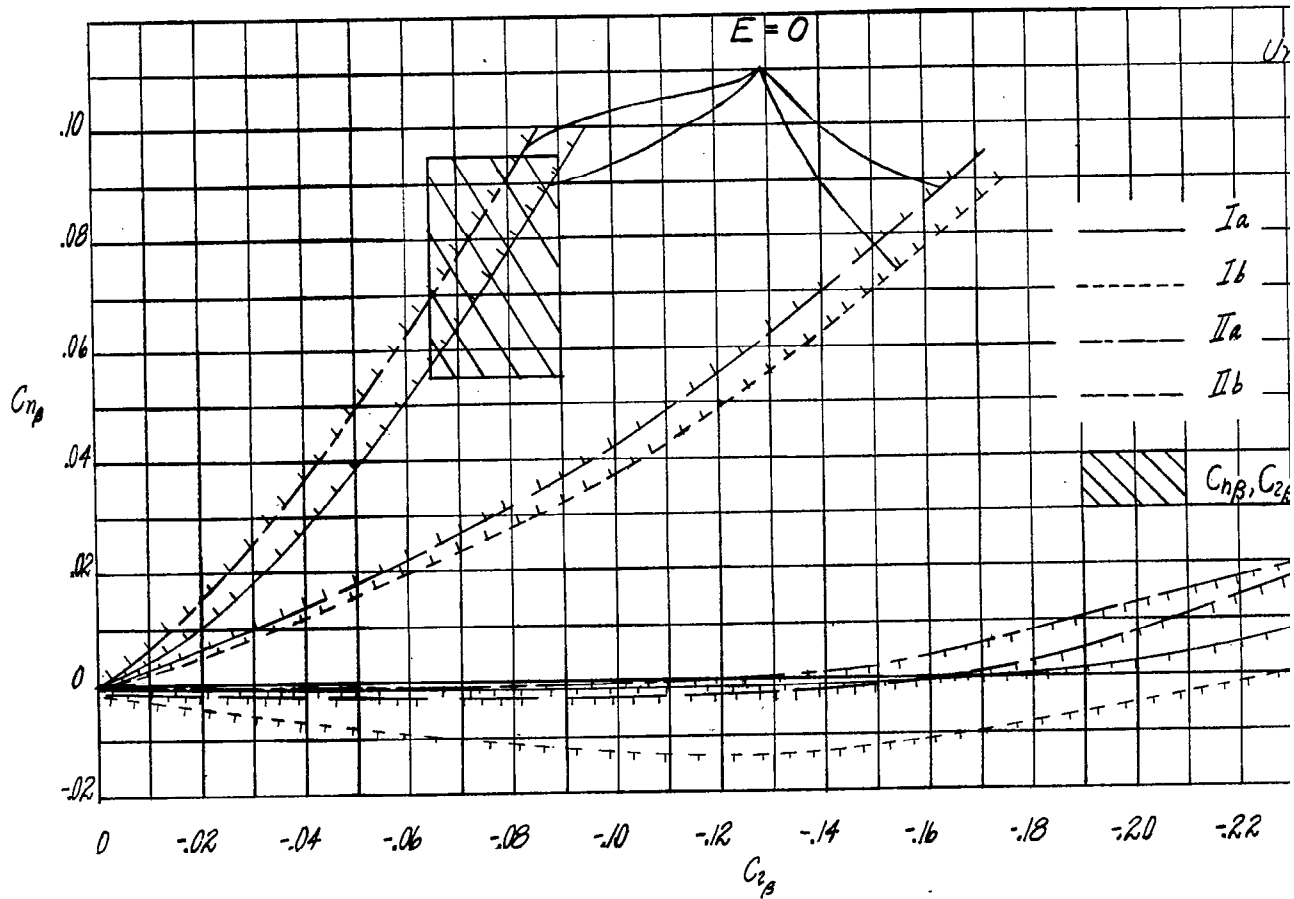
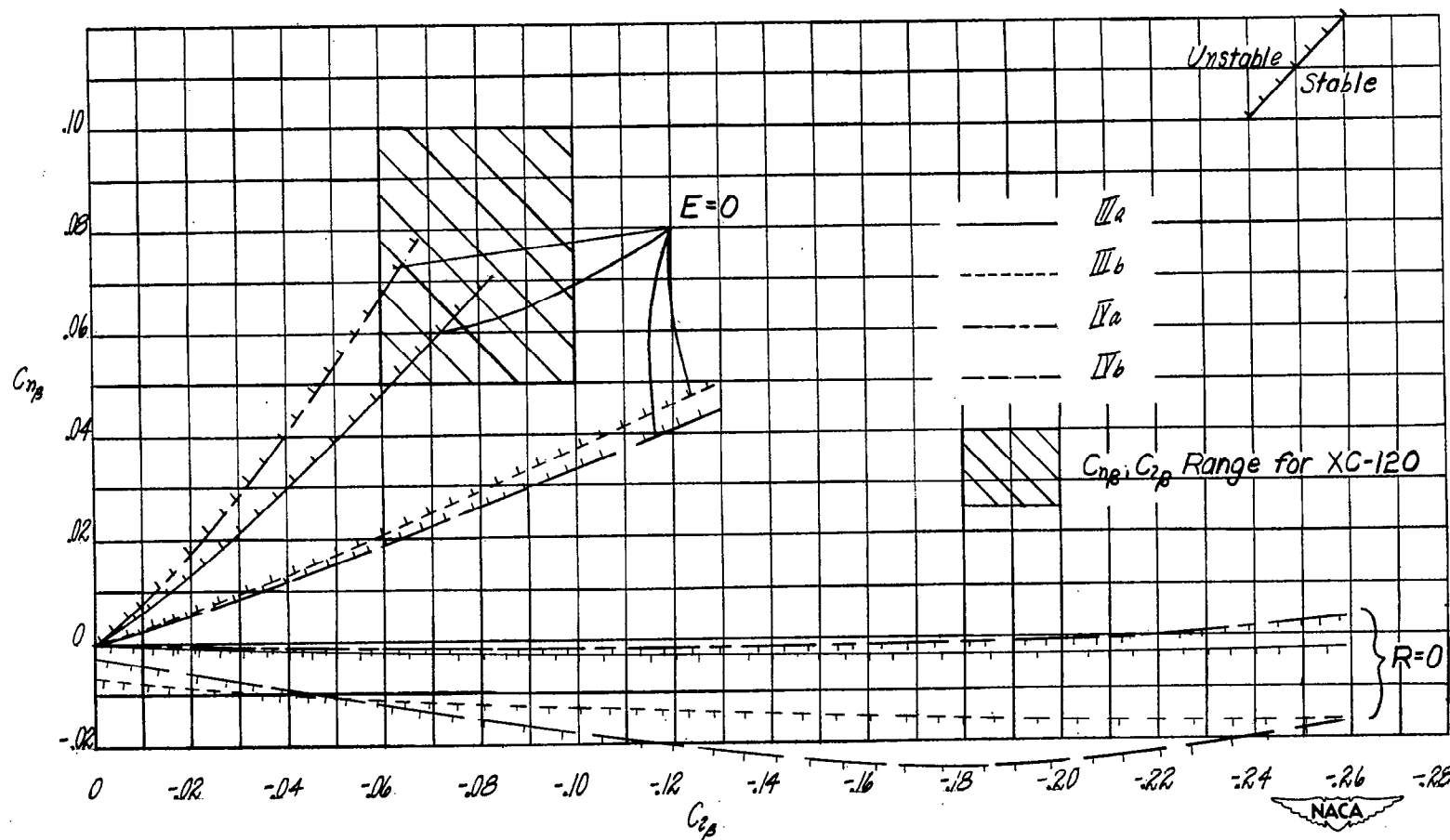


Figure 1.- Three-view sketch of the XC-120 airplane.



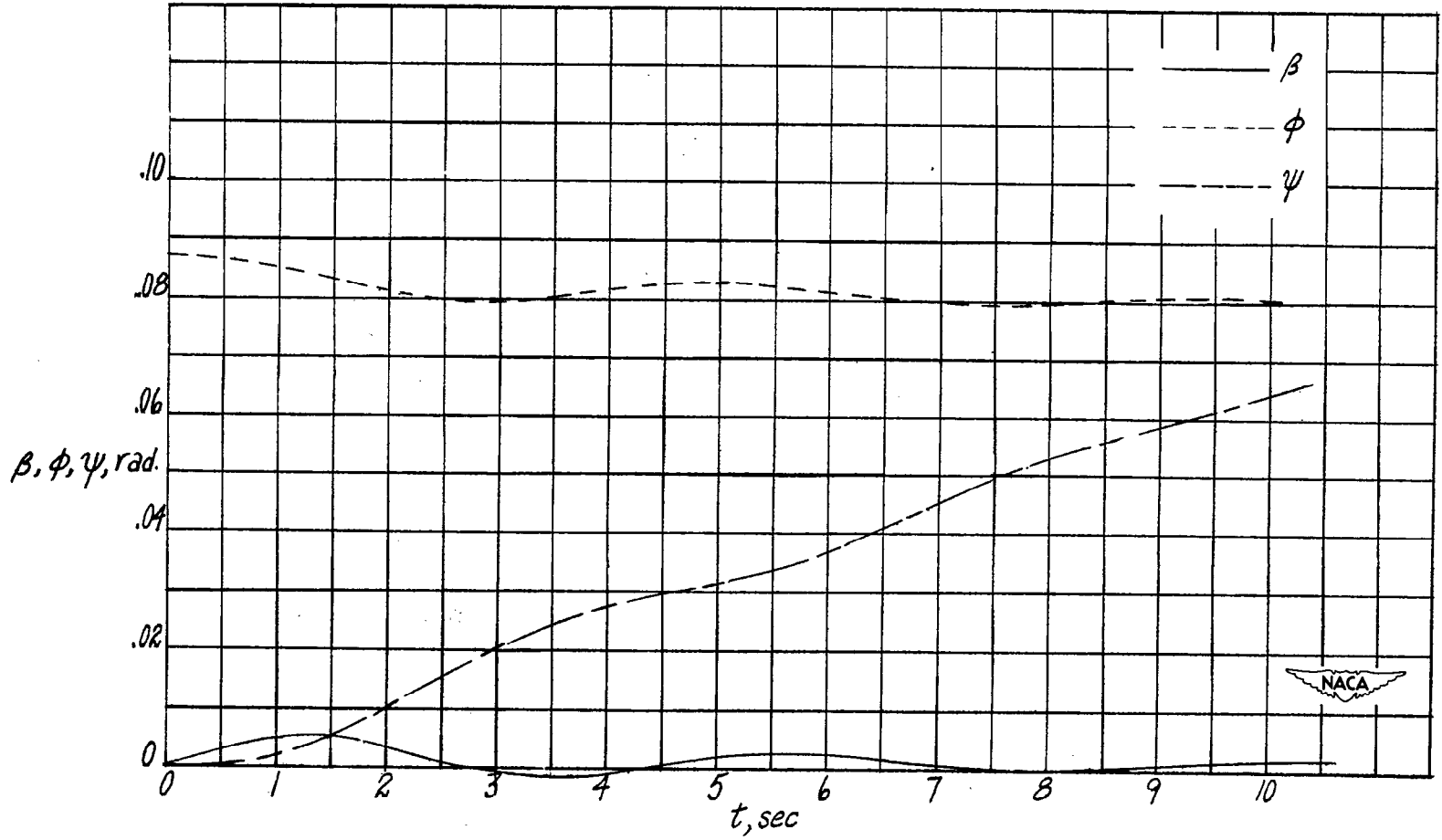
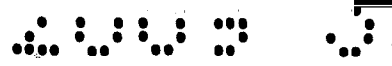
(a) Cruising condition.

Figure 2.- Lateral-stability boundaries for the XC-120 airplane.



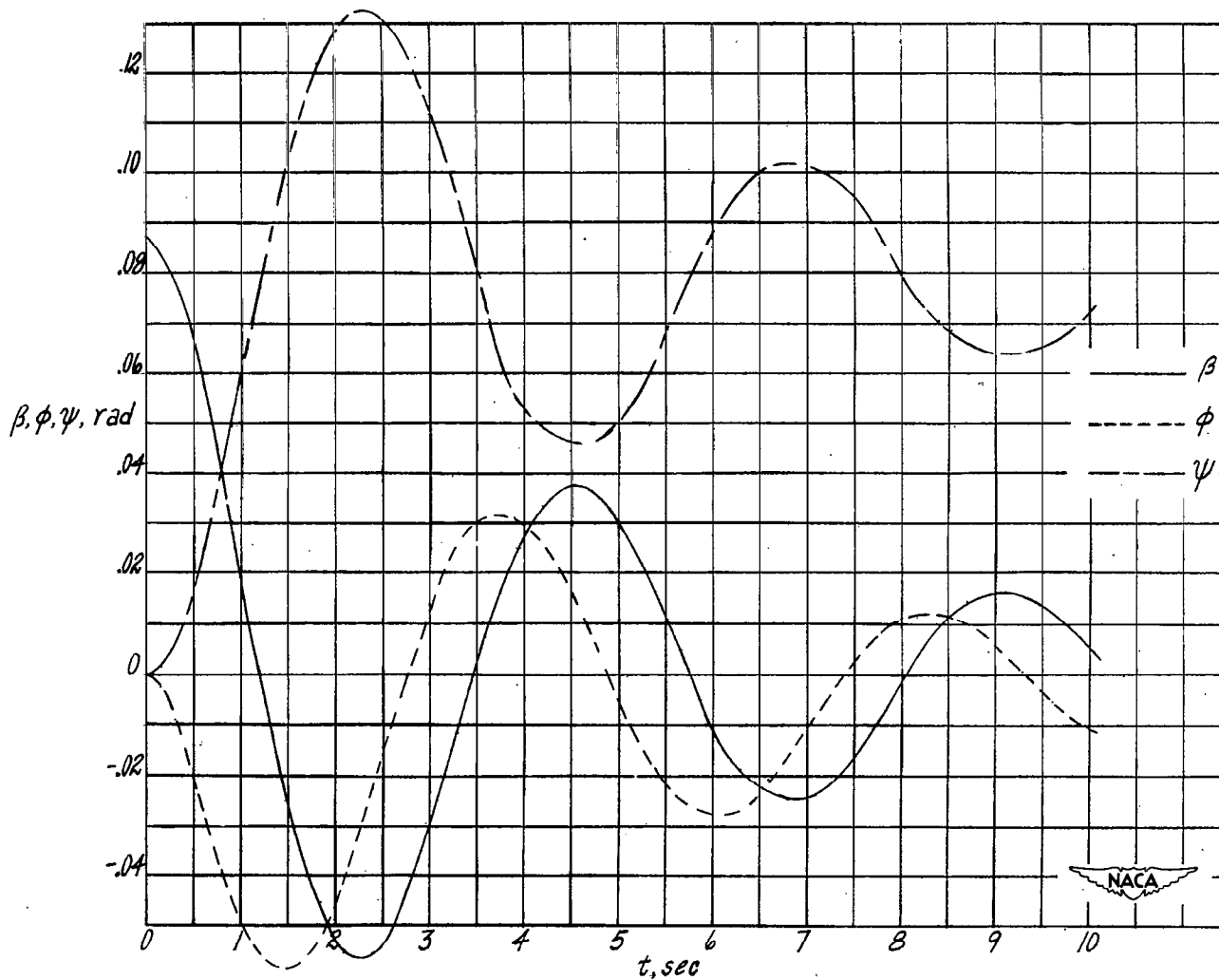
(b) Landing condition.

Figure 2.- Concluded.



(a) Motion subsequent to a displacement in bank.

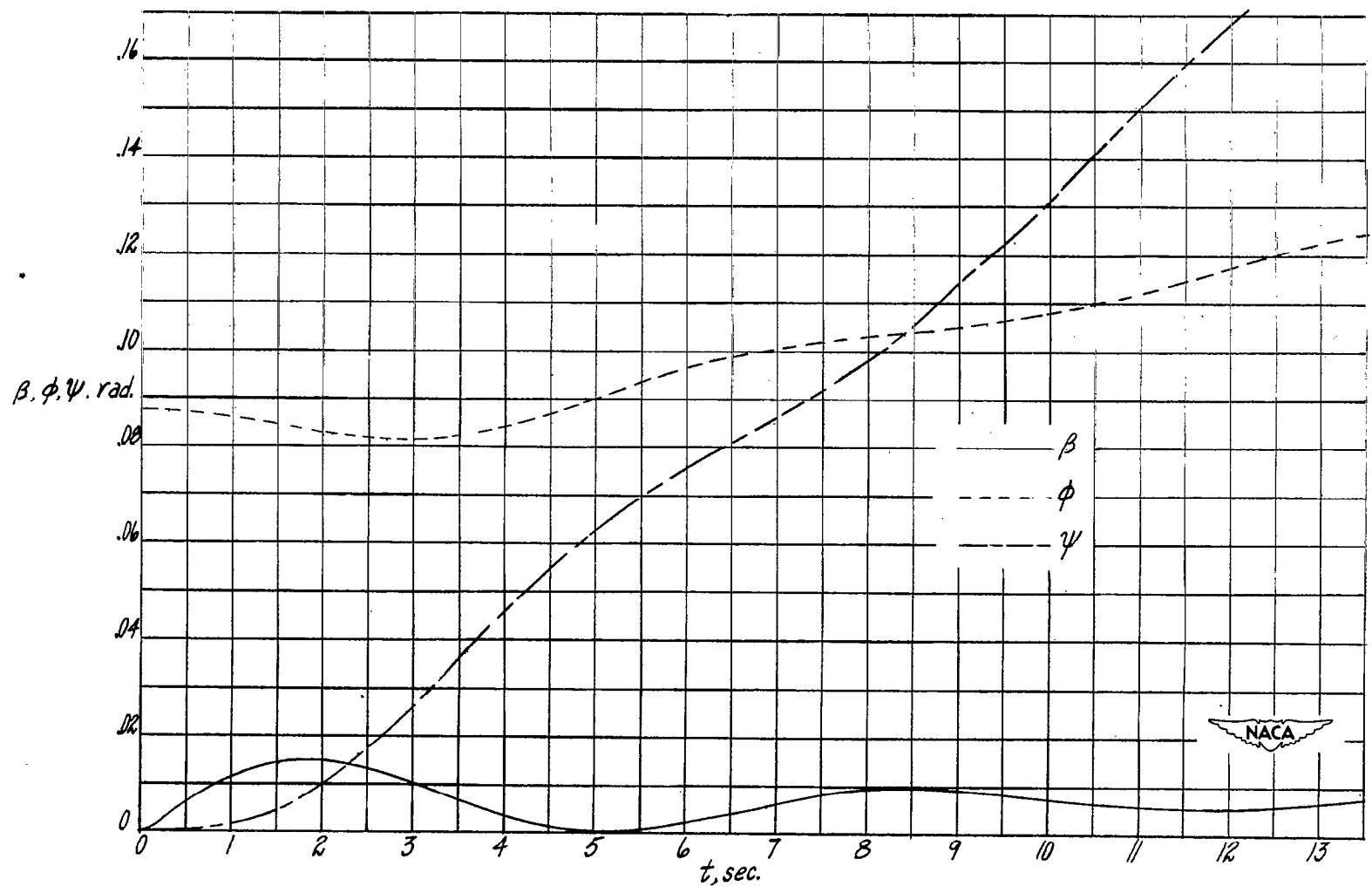
Figure 3.- Lateral motions of the XC-120 airplane. Case IIa.



(b) Motion subsequent to a displacement in sideslip.

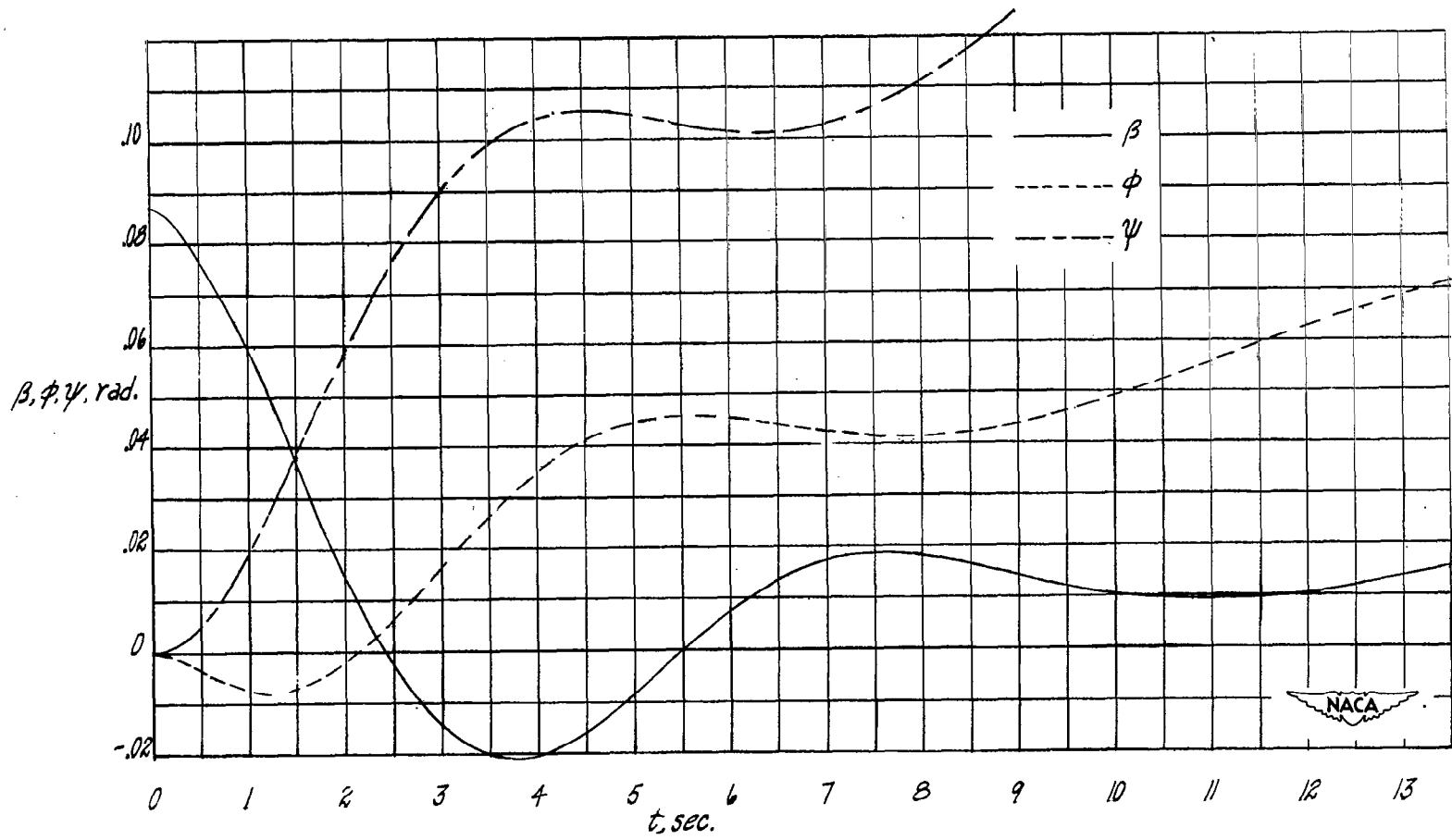
Figure 3.- Concluded.





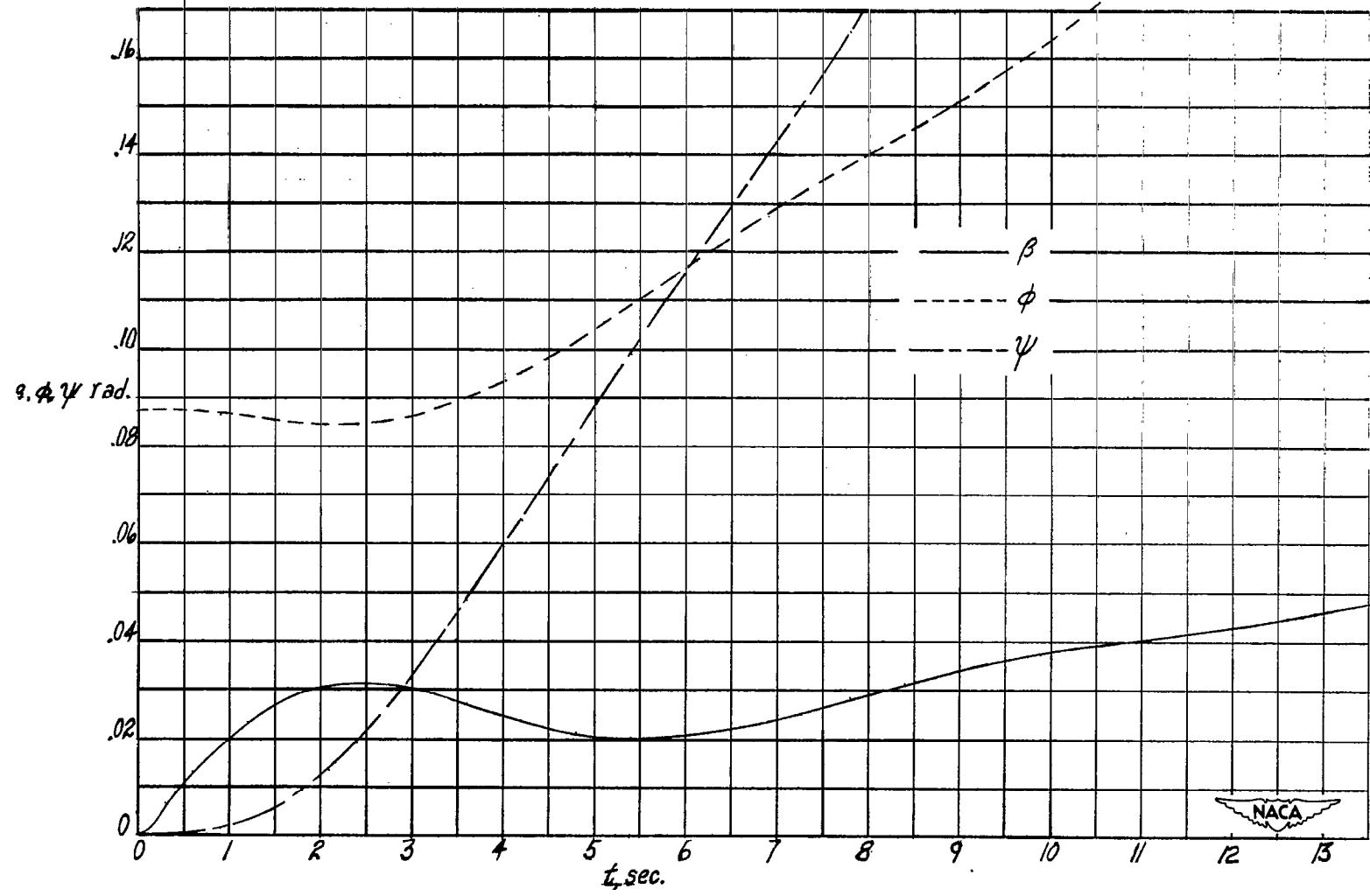
(a) Motion subsequent to a displacement in bank.

Figure 4.- Lateral motions of the XC-120 airplane. Case IIb.



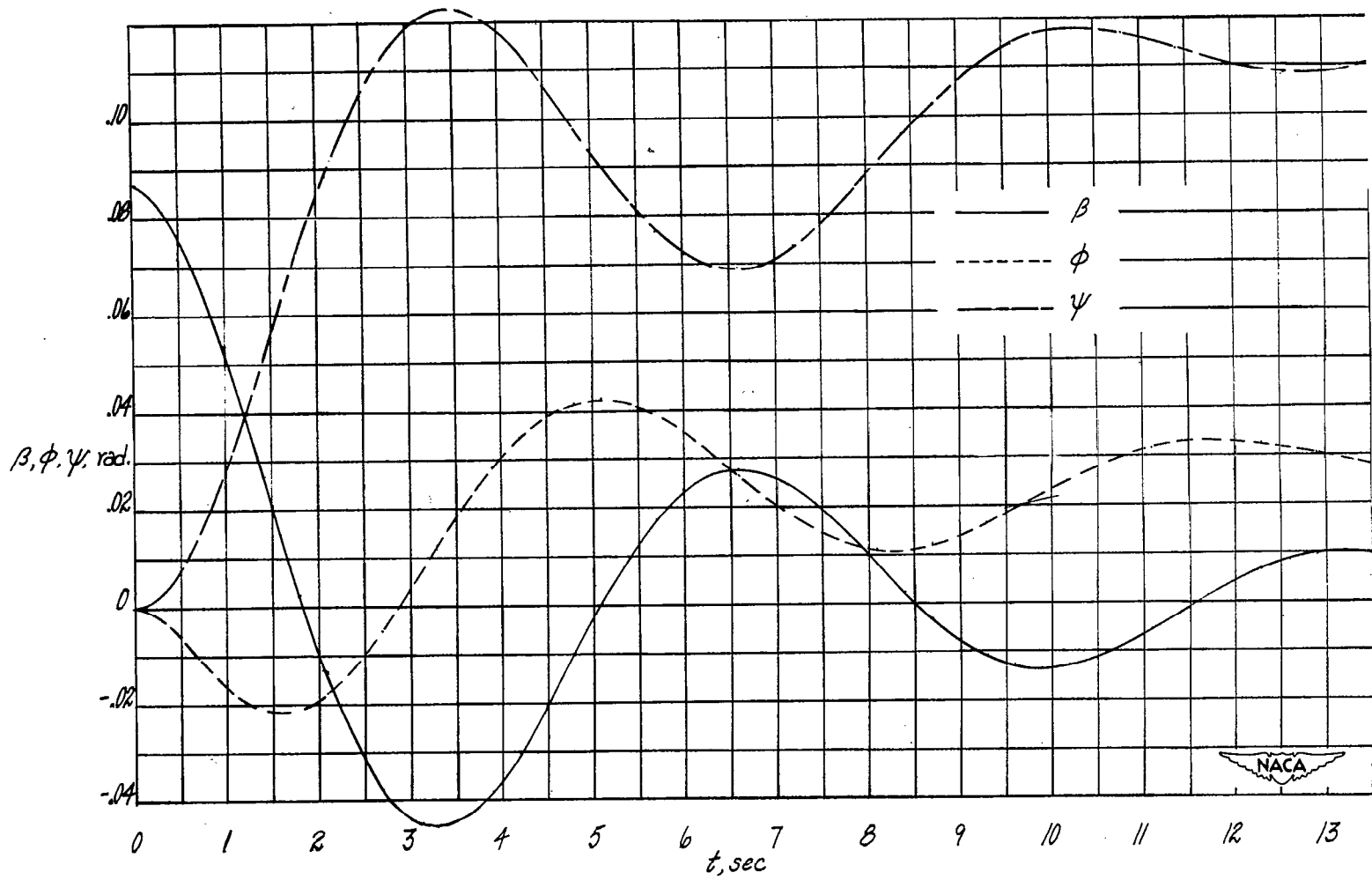
(b) Motion subsequent to a displacement in sideslip.

Figure 4.- Concluded.



(a) Motion subsequent to a displacement in bank.

Figure 5.- Lateral motions of the XC-120 airplane. Case IVb.



(b) Motion subsequent to a displacement in sideslip.

Figure 5.- Concluded.

NASA Technical Library



3 1176 01437 9755